Published in final edited form as:

Mol Cancer Res. 2022 October 04; 20(10): 1548–1560. doi:10.1158/1541-7786.MCR-22-0026.

EPAC Regulates Melanoma Growth by Stimulating mTORC1 Signaling and Loss of EPAC Signaling Dependence Correlates with Melanoma Progression

Aishwarya Krishnan[1,*], **Aishwarya I. Bhasker**[1,*], **Mithalesh K. Singh**[1,*], **Carlos. I. Rodriguez**[1,#], **Edgardo Castro-Pérez**[1,¶], **Sarah Altameemi**[1], **Marcos Lares**[1], **Hamidullah Khan**[1], **Mary Ndiaye**[1], **Nihal Ahmad**[1,2], **Stefan M. Schieke**[1,2], **Vijayasaradhi Setaluri**[1,2,§]

[1]Department of Dermatology, University of Wisconsin School of Medicine and Public Health, University of Wisconsin-Madison, WI, 53705

[2]William S. Middleton Memorial Veterans Hospital, Madison, WI, 53705

Abstract

Exchange Proteins directly Activated by cAMP (EPACs) belong to a family of RAP guanine nucleotide exchange factors (RAPGEF). EPAC1/2 (RAPGEF3/4) activate RAP1 and the alternative cAMP signaling pathway. We previously showed that the differential growth response of primary and metastatic melanoma cells to cAMP is mediated by EPAC. However, the mechanisms responsible for this differential response to EPAC signaling are not understood. In this study, we show that pharmacological inhibition or siRNA-mediated knockdown of EPAC selectively inhibits the growth and survival of primary melanoma cells by downregulation of cell cycle proteins and inhibiting the cell cycle progression independent of ERK1/2 phosphorylation. EPAC inhibition results in upregulation of AKT phosphorylation but a downregulation of mTORC1 activity and its downstream effectors. We also show that EPAC regulates both glycolysis and oxidative phosphorylation, and production of mitochondrial reactive oxygen species, preferentially in primary melanoma cells. Employing a series of genetically matched primary and lymph node metastatic (LNM) melanoma cells, and distant organ metastatic melanoma (MM) cells, we show that the LNM and MM cells become progressively less responsive and refractory to EPAC inhibition suggesting loss of dependency on EPAC signaling correlates with melanoma progression. Analysis of TCGA dataset showed that lower RAPGEF3, RAPGEF4 mRNA expression in primary tumor is a predictor of better disease-free survival of patients diagnosed with primary melanoma suggesting that EPAC signaling facilitates tumor progression and EPAC is a useful prognostic marker. These data highlight EPAC signaling as a potential target for prevention of melanoma progression.

[§]Address for Correspondence: Vijayasaradhi Setaluri, PhD, Department of Dermatology, Wisconsin Institute for Medical Research, 1111 Highland Avenue, University of Wisconsin-Madison, Madison, WI, 53706; Phone: (608) 263-5362, vsetaluri@dermatology.wisc.edu.

[*]These authors contributed equally

[#]Current address: Department Pathology, University of California San Francisco, San Francisco, California;

[¶]Current address: Center for Molecular Biology and Cell Disease, Instituto de Investigaciones Cientificas y Servicios de Alta Tecnologia, Panamá, Panama

Conflict of Interest: The authors do not have any conflict of interest and do not have any disclosures

INTRODUCTION

Cutaneous melanoma arises form epidermal melanocytes. If diagnosed early, excision of the primary tumor in the skin can be curative. However, the five-year survival rates decrease precipitously as melanoma metastasizes [1, 2]. Melanoma tumor progression models often describe a sequence of steps in melanomagenesis from proliferation of malignant melanocytes, nevus development to dysplastic nevus to melanoma *in situ* (also known as radial growth phase) to vertical growth phase or invasive melanoma [3]. Tumor progression from locally invasive lesion to metastatic tumor is thought to occur through lymphatics, followed by systemic metastasis through the blood [4, 5]. Accordingly, the evidence-based revision of the AJCC melanoma staging system includes presence of microsatellites, satellites, or in-transit metastases and the number of tumor-involved regional lymph nodes [6]. However, molecular mechanisms involved in primary melanoma tumor evolution that promote lymphatic invasion are not completely understood [7].

In previous studies, we showed that EPAC (Exchange Protein directly Activated by cAMP) signaling is required for the growth and survival of primary melanoma but not metastatic melanoma [8] suggesting that loss of dependency on EPAC signaling correlates with tumor progression. EPAC, also known as RAPGEF or cAMP-GEF, is a guanine nucleotide exchange factor that activates RAP1/2 from a GDP-bound inactive state to GTP-bound active state [9]. EPAC family of proteins, consisting of one isoform of EPAC1 and three isoforms of EPAC2, activate the alternative cAMP signaling pathway. Although a role for EPAC signaling in variety of cancers has been reported [10–15], the exact mechanisms of action of EPAC in melanoma have not been investigated. For example, overexpression of EPAC in bladder cancer cells was reported decrease their migration [10]. On the other hand, pharmacological inhibition of EPAC appears significantly decrease migration of pancreatic cancer cells [16]. In some ovarian cancer cells EPAC was shown to play a pro-migratory role and anti-migratory role in some others [17–19]. EPAC2 was found to inhibit HDAC8 protein degradation by the inhibition of the PI3K-AKT pathway through the EPAC2-Rap1 signaling axis in non-small cell lung cancer NSCLC [20]. EPAC was also found to promote angiogenesis in endothelial cells by upregulating VEGF receptor-2 (VEGFR-2) [21].

In this study, employing a series of genetically matched primary and lymph node metastatic melanoma cells (LNM), and pharmacological and genetic inhibition of EPAC, we show that EPAC signaling promotes cell cycle progression and growth selectively in primary melanoma cells. This dependency of primary melanoma cells on EPAC is independent of oncogenic driver mutation and is mediated by mTORC1 signaling. We also show that LNM cells and distant metastases become progressively less dependent on EPAC signaling. Analysis of a TCGA melanoma dataset showed that EPAC expression is a useful prognostic marker. and a potential therapeutic target to prevent melanoma progression. Our data suggest that EPAC is a potential therapeutic target to prevent melanoma progression and understanding the mechanisms of resistance of metastatic melanoma to EPAC inhibition could open new avenues for treatment of melanoma.

MATERIAL AND METHODS

Cell culture

WM series primary and metastatic cells were from Rockland Immunochemicals (Limerick, PA) and cultured in tumor specialized medium (TSM) containing 2% heat inactivated fetal bovine serum (FBS) and 1% penicillin and streptomycin. Matched primary and lymph node metastatic (LNM) cell lines were verified by Short Tandem Repeat (STR) analysis by the Cell Line Authentication Service of UW TRIP Lab. MRA series metastatic melanoma cell lines, established at UW-Madison by Dr. Mark Albertini, were cultured in DMEM with 10% FBS and 1% penicillin and streptomycin. All cells were cultured in a humid incubator at 37°C with 5% CO_2. Cells were routinely checked for mycoplasma contaminations using the Universal Mycoplasma PCR Detection Kit (ATCC, Manassas, VA) according to the manufacturer's instructions. Cells were used form passage #4 to #12. Details of all the cell lines used in this study are listed in Supp Table S1.

Chemicals and antibodies

The EPAC inhibitor ESI-09 and the AKT inhibitors AZD5363 were acquired from Selleckchem (Houston, TX). Rp-8-bromo-Cyclic AMPS and 8-pCPT-2'-O-Me-Cyclic AMP were acquired from Cayman Chemical (Ann Arbor, Michigan). MitoSOX Red was obtained from Thermo Fisher Scientific. Sources and dilution of antibodies used are listed in Supp Table S2.

Western blotting

Cells were washed, scraped, and lysed using RIPA buffer containing Halt protease inhibitor cocktail (Thermo Fisher Scientific) and phosphatase inhibitor cocktail (Thermo Fisher Scientific). For proteins sensitive to degradation, cells were lysed directly on the plate using lysis buffer. Samples were then sonicated, centrifuged for 30 mins at 4°C and the supernatants were collected. Protein concentration was estimated (Pierce BCA Protein Assay Kit, Thermo Fisher Scientific) and 20-40μg of protein was analyzed by SDS-PAGE followed by transfer to PVDF membrane. Membranes were blocked with 5% nonfat dry milk in 0.1% Tween in Tris-buffered Saline. Primary and secondary antibody dilutions for immunoblotting were used as shown in Supp Table S2. Blots were imaged using Pierce ECL Western Blotting Regent (Thermo Fisher Scientific).

MTT Assays

In a flat-bottomed 96-well plate, 5000 cells per well were plated for MTT assays. Cells were cultured at 37°C overnight before being treated with various chemical agents for the times mentioned in the legends of the figures. At the endpoint, 20l of 5mg/ml Thiazolyl Blue Tetrazolium Bromide (MTT; Sigma-Aldrich) was added to the wells, plates were incubated for 1 hour at 37°C, and absorbance at 540nm was measured using a Biotek Synergy H1 Multi-Mode Plate Reader. For MTT assays, we employed another kit (#11465007001, Sigma-Aldrich, MA) according to the manufacturer's instructions.

Clonogenic Assay

For clonogenicity assays, 1000 cells/well were pated in triplicates in 6-well plates. Cells were incubated at 37°C overnight, followed by treatment with media containing drug, every 4 days for 2-3 weeks (or until visible colonies were observed). The plates were washed with 1X PBS, stained, and fixed with 0.5% crystal violet in 70% ethanol for 1h and colonies were counted.

EPAC1/2 siRNA Knockdown

Cells were transfected with two different siRNAs for EPAC1/RAPGEF3 (#4392420, s1# s20362, s2#s20360, Ambion, Thermo Fisher Scientific) and EPAC2/RAPGEF4 (#4392420, ID # s21814, ID #s21816, Ambion, Thermo Fisher Scientific). Equal number of cells were plated (2×10^5 cells/ml) in a 6-well plate 24h prior to transfection. Cells were transfected with a fluorescein (Cy5) conjugated control siRNA (#SIC005, Sigma Aldrich) or with the pooled siRNAs (30μM total concentration, 15μM for each siRNA,) using Lipofectamine™ RNAiMAX (Thermo Fisher Scientific). The transfection mixture was prepared in antibiotic-free Opti-MEM. Media was changed 16h post-transfection and harvested after 96h for Western blot analysis.

EPAC1 and EPAC2 overexpression

We obtained MYC tagged-EPAC1 from Dr. Stephen J Yarwood of Heriot-Watt University, Edinburgh, UK and DDK tagged-EPAC2 (#RC205335) from Origene (Rockville, MD). $2.5x10^5$ cells/ml in triplicate wells in 6-well plates were transfected with 5μg empty vector plasmid (#PCMV6NEO, Origene, Rockville, MD) or MYC tagged-EPAC1 or DDK tagged-EPAC2 plasmids using Lipofectamine™ RNAiMAX (Thermo Fisher Scientific, Waltham, MA) in reduced serum Opti-MEM. The medium was changed 16 hours post transfection, and the cells were maintained in Geneticin (G418 2.5mg/ml) containing medium. Cells were lysed 5 days post- transfection and protein expression was analyzed by western blot using anti-Myc and ant-DDK antibodies. Bulk transfected cells were trypsinized and plated in 6 replicate wells (5,000 cells/well) in multiple 96-well plates and the cell growth was assessed using MTT assay.

Lentiviral RAP1GAP Knockdown

HEK293 cells were transfected with a control empty vector pLKO.1 (SHC001V) or a pool of three RAP1GAP short hairpin RNA (shRNA) plasmids (sc-36388-SH) (Santa Cruz Biotechnology, Dallas, TX). Competent lentiviruses were collected 48h and 96h after transfection and the titer estimated (Quick Titer Lentivirus Titer Kit, Cell Biolabs, San Diego, CA) as directed by the manufacturer. For transduction, cells were plated at 50% confluence, then viral media with 5μg/ml polybrene were added to cells five times over two days. After 48 h of transduction, the medium was replaced, and cells were maintained in puromycin (2.5μg/ml) containing medium.

RAP1-GTP pulldown assay

Cells were lysed with RIPA buffer with protease and phosphatase inhibitors. The pull down was performed as described [22] using Active Rap1 Pull-Down and Detection Kit (Sigma-

Aldrich, St. Louis, MO). Briefly, cell lysates were incubated with GST-Rap-binding domain (RBD) and then pulled down using anti-GST antibody and used to validate anti-Active RAP1 antibody (New East Biosciences, Malvern, PA).

Subcellular Fractionation

Cells ($1x10^6$) were plated in 100mm dish in complete culture medium and the fractionated using Subcellular Protein Fractionation Kit (Thermo Fisher Scientific) according to the manufacturer's instructions. Briefly, cells were harvested by trypsinization, pelleted, and incubated in ice-cold cytoplasmic extraction buffer containing protease inhibitors at 4^0C for 10 min with gentle mixing. The lysate was centrifuged for 5 min at 500 x g and kept at 4^0C. The supernatant (cytoplasmic extract) was transferred to a fresh ice-cold tube. To the pellet, membrane extraction buffer was added and vortexed for 10s. The suspension was incubated at 4^0C for 15 min with gentle mixing, centrifuged for 10 min at 3000 x g and kept at 4^0C and the supernatant containing membrane proteins was collected. The remaining pellet was then extracted in ice-cold nuclear extraction buffer by vortexing for 15s and incubation for 30 min at 4^0C. The mixture was centrifuged for 15 min at 5000 x g and kept at 4^0C and the supernatant was collected as a soluble nuclear extract. The protein concentration was estimated and 30μg was used for SDS-PAGE and western blotting.

Immunocytochemistry

Cells were plated on 8-well slides (Ibidi, USA, #80826) and after 24hours cells were treated with DMSO or ESI-09 for 24hours. Next day, the cells were fixed in 4% paraformaldehyde in PBS for 15 min. Fixed cells were treated with 0.3% H_2O_2 for 10 min followed by incubation in Ultra V Block (UltraVision LP Detection System, Thermo Fisher Scientific) for 10 min at room temperature and then in permeabilization/blocking buffer (0.3% Triton X-100, 1% BSA, and 10% normal donkey serum in PBS) for 45 minutes. The slides were incubated with anti-RAP1GAP antibody (Santa Cruz, Dallas, TX1:1000) or anti-active RAP1 mouse polyclonal antibody (New East Biosciences; 1:1000) diluted in permeabilization/blocking buffer overnight at 4^0 C. Next day, cells were washed 3 times with 1% BSA in PBS for 5 min and antibody binding was detected using UltraVision LP Detection System according to the manufacturer's recommendations and cells were counterstained with hematoxylin.

Flow Cytometry

Cells were plated ($2\text{-}4x10^5$ cells/100mm plate) in triplicates and synchronized by thymidine double block. Cells were treated to 2mM thymidine (Sigma-Aldrich) for 14 h followed by thymidine-free medium for 5 h and then thymidine was added again for 14h. Cells were treated with DMSO or ESI-09 up to 48 h. Cells were trypsinized, pelleted, washed with 1X PBS and resuspended in 1ml of 1X PBS. 2 volumes of pre-chilled ethanol were added to the cells on vortex and stored at 4°C overnight. Samples were then stained overnight in dark with propidium iodide (500μg/ml PI plus 100μg/ml RNase A in PBS).

Mitochondrial ROS assay

Cells ($2.5x10^5$) were plated in triplicates in 6-well plates for each treatment. After overnight incubation of cells at 37°C, the growth medium was replaced with medium containing DMSO or 2.5 μM ESI-09. After 48h of treatment, cells were trypsinized, suspended in DMEM (with fetal bovine serum, penicillin, and streptomycin), centrifuged, and the pellet resuspended in 1ml HBSS. MitoSOX Red (5μM) was added to the suspension and incubated at 37°C in dark for 10 min. Cells were centrifuged, washed twice with HBSS, and analyzed in a flow cytometer.

Seahorse Cell Energy Phenotype test

Cells were plated at 80% confluence in a Seahorse XF96 cell culture microplate. After 16 hours, medium was replaced with medium containing DMSO or ESI-09. After 24 hours, medium was replaced with Seahorse XF assay medium pH 7.4 (unbuffered DMEM containing 200 mM GlutaMax-I and glucose) and the plate was incubated at 37°C for 1 hour. Baseline and maximal oxygen consumption rates and extracellular acidification rates were measured using XFp Extracellular Flux Analyzer (Agilent, Santa Clara, CA). The stressor mix contained FCCP (0.5 μM), an oxidative phosphorylation uncoupler and oligomycin (1 μM), an ATP synthase inhibitor.

Analysis of The Cancer Genome Atlas (TGCA)

Dataset from TCGA was retrieved using cBioPortal containing the mRNA expression and clinical information of 479 melanoma patients (TCGA, Firehose Legacy, accessed on November 25, 2021) [23, 24]. This cohort contained 100 patients that were diagnosed with primary melanoma in which 86 had complete clinical follow up. We analyzed the mRNA expression of *RAPGEF3, RAPGEF4, RAP1GAP, mTOR* genes and disease-free survival (DFS) of these primary melanoma patients. Patients were stratified into 4 quartiles based on the expression of each mRNA and survival analysis was performed using low (quartiles 1-3) and high mRNA (quartile 4). The Kaplan–Meier curves between these two groups were plotted by GraphPad Prism (v9.3.1).

Statistical Analysis

All statistical analyses were performed using GraphPad Prism v 9.3.1. Flow cytometry data was analyzed using Modfit 9.0.

RESULTS

EPAC plays a differential role in growth of primary and metastatic melanoma cells

First, we determined the endogenous levels of EPAC 1 and EPAC 2 proteins in normal human primary melanocytes, primary and metastatic melanoma cell lines by western blot analysis. Expression of EPAC 1 and 2 proteins is upregulated in melanoma cells compared to melanocytes. Mouse brain tissue extract served as positive control [25] (Fig 1A). We studied the effect of pharmacological inhibition of EPAC on the growth of melanoma cells. ESI-09 is a non-cyclic nucleotide that inhibits the guanine nucleotide exchange factor activity of both EPAC1 and EPAC2 [16]. Treatment with ESI-09 inhibited the growth of all

primary melanoma cell lines tested irrespective of the oncogenic mutation they harbor (Fig 1B, **top panels and** Supp Table 1), but mildly stimulated the growth of metastatic melanoma cells (Fig 1B, **bottom panels**). To understand whether the switch from a growth promoting function of EPAC in primary melanoma to the growth inhibitory function in metastatic melanoma cells is associated with tumor progression, we assessed the effect of ESI-09 on primary and metastatic melanoma cell lines established from the same patient. The cell lines WM115, WM266-4, WM239A and WM165-1 were all derived from melanocytic lesions in the same patient; WM115 originated from the VGP primary tumor and WM266-4, WM239A and WM165-1 were established from individual lymph node metastases (LNM) that were progressively distant from the VGP primary melanoma [26] . Treatment of primary melanoma cells WM115 with ESI-09 inhibited their growth, whereas this inhibitory effect is less pronounced, progressively, in the LNM cell lines WM266-4, WM239A and WM165-1 (Fig 1C). This differential effect of EPAC inhibitor on primary and metastatic cells is also evident from dose-response curves (Fig 1D). Sustained inhibition of EPAC also inhibited the clonogenicity of primary and WM165-1 LNM cells but not distant metastatic melanoma cells (Fig 1E) suggesting that primary melanoma cells require the activity of EPAC for growth and proliferation whereas EPAC can act as a negative regulator of growth of metastatic melanoma cells. Next, we asked whether the effects of pharmacological inhibition of EPAC is reversible. We treated primary melanoma cells (WM1552C, WM1862 and WM115) with ESI-09 for 8, 24 or 48 hours and replaced the medium with fresh inhibitor-free medium and cultured the cells for a total of 5 days from the time of initial treatment with the inhibitor. Data in (Supp. Fig. S1A) show that the effect of ESI-09 was partially reversible up to 24h of treatment with the inhibitor. However, after 24h treatment, the effect of ESI-09 on the growth of primary melanomas was not reversible.

To validate this differential response of primary and metastatic melanoma cells to pharmacological inhibition of EPAC, we performed knockdown (KD) of EPAC1 or EPAC 2 or both EPAC1/2 by transfection of primary (WM1552C) and metastatic (MRA6) melanoma cells with EPAC1 and EPAC2 two separate siRNAs (Fig. 2A). EPAC1 KD inhibited growth of WM1552C cells by approximately 30% and while EPAC2 KD decreased their growth by approximately 70% (Fig 2B). However, KD of neither EPAC1 nor EPAC2 had any significant effect on the growth of the metastatic MRA6 cell. Further, knockdown of both EPAC 1/2 showed that survival of primary but not metastatic melanoma cells is dependent on EPAC.

To investigate whether overexpression of EPAC1 or EPAC2 also preferentially enhance the growth of primary melanoma cells, we transfected primary and metastatic melanoma cells with empty vector or EPAC1 or EPAC2 expression plasmids. Overexpression of either EPAC1 or EPAC2 significantly increased the growth of WM1552C primary melanoma cells consistent with the data from knockdown experiments. In contrast, overexpression of EPAC1 did not affect the growth of the MRA6 metastatic melanoma cells while overexpression of EPAC2 resulted in slight growth inhibition (Fig. 2C).

Next, using the matched primary and LNM cell lines WM115, WM266-4, WM239A and WM165-1, we tested the effect of a EPAC2-selective inhibitor ESI-05 [34] to investigate the relative contribution of EPAC1 and EPAC2. Treatment of primary melanoma cells (WM115)

with ESI-05 decreased their growth whereas a similar treatment with the EPAC2-selective inhibitor had no effect on the growth of the LNM cell lines (WM266-4, WM239A and WM165-1) (Fig. 2D). Treatment with EPAC inhibitors ESI-05 or -09 also inhibited the growth of mouse primary melanoma cell lines YUMM3.3 and YUMM1.7 (Supp Fig. S1B). These data show that EPAC (predominantly EPAC2) signaling is required for growth and survival of primary melanoma cells.

To investigate the role of cAMP in EPAC action, we evaluated the effect of a cAMP analog and a selective EPAC activator, 8-pCPT-2′-O-Me-cAMP (8-pCPT-cAMP), and a cAMP antagonist, 8-Bromoadenosine-3′,5′-cyclic mono-phosphoropthioate (Rp-8-Br-cAMP), which inhibits both PKA and EPAC signaling, on the growth of matched primary and LNM cell lines and two metastatic melanoma cell lines (Supp. Fig S1C). Treatment with the cAMP analogue had no effect on the growth of primary melanoma cells (WM115) but inhibited the growth of LNM cells WM165-1 and metastatic melanoma cells MRA5, MRA6. On the other hand, treatment with the cAMP antagonist Rp-8-Br-cAMP inhibited the growth of primary and LNM cells, but not metastatic melanoma cells. These data suggest that in primary cells EPAC signaling is maximally activated independent of exogenous cAMP levels.

Inhibition of EPAC activity delays cell cycle progression

Next, we asked whether growth inhibition by ESI-09 selectively in primary melanoma cells is due to cell cycle progression. We synchronized the cell cycle of primary WM1552C, WM1862, and metastatic MRA6 melanoma cells by double thymidine block and then treated with ESI-09. As shown in Fig 3A–B, 24h after release from thymidine block, cell cycle progression of DMSO treated WM1552C cells resulted in a distribution of 43% in S phase and 36% cells G2/M phase, whereas the entire population of ESI-09 treated cells remained in G1 phase of cell cycle. Metastatic MRA6 melanoma cells exhibit accelerated cell cycle progression after double thymidine block and release (compare 12h DMSO treated WM1552C and MRA6). However, treatment of MRA6 cells with ESI-09 did not significantly alter their cell cycle progression (Fig 3C–D).

Western blot analysis of cell cycle regulators showed that treatment with ESI-09 resulted in downregulation of cyclin D1 and CDK4 in primary melanoma cells WM1552C, WM1862. CDK inhibitors, p21 and p27, which are sequestered by the cyclin D-CDK4 complex, and cyclin B, which regulates the transition from G2 into M phase were also downregulated (Fig 3E, **left panel**). No change in the levels of these proteins was evident in metastatic melanoma cell lines MRA5 and MRA6 (Fig 3E, **right panel**). Treatment with ESI-09 did not affect the levels of other cell cycle regulatory proteins CDK6, p15, CDK2, Cyclin A and Cyclin E (Supp Fig. S2A). Western blot analysis of cell cycle proteins in two sets of matched primary and LNM cells also showed that ESI-09 treatment downregulated cell cycle regulators consistent with the pattern of growth inhibition by ESI-09 (Fig 3E & Fig. S2B). These data shows that EPAC signaling promotes cell cycle progression in primary melanoma cells.

To investigate whether apoptotic cell death contributes to the observed inhibition of primary melanoma cells, we assessed the effect of a pan-caspase inhibitor, Z-VAD-FMK, on the

effect of ESI-09. As shown in (Supp Fig S3), treatment of BRAF(V600E) mutant primary and metastatic melanoma cells with the BRAF inhibitor PLX4032 (BRAFi), decreased cell survival by 60% and 45%, respectively, and addition of z-VAD-FMK 8h after treatment with the BRAFi significantly rescued their survival. Survival of primary melanoma cells treated with ESI-09 decreased by 30% and in the presence of the caspase inhibitor this decrease was 15% showing that treatment with ESI-09 also activates apoptosis. ESI-09 had no effect on survival of metastatic melanoma cells and interestingly addition of the caspase inhibitor resulted in a small but significant decrease in their survival (Supp Fig. S4). These data suggest cell cycle inhibition and apoptosis contribute to the growth inhibition of primary melanoma cells treated by the EPAC inhibitor ESI-09.

Role of RAP1GAP signaling in primary and metastatic melanoma

In previous studies[8], we showed that treatment with ESI-09 results in downregulation of active RAP1(RAP1-GTP) in both primary and metastatic melanoma cells (Supp Fig. S5 & S6). RAP1-GTP levels are regulated by the activity of EPAC, which is a RAP guanosine exchange factor (RAPGEF) and RAP1GAP, which is a GTP hydrolyzing enzyme. To understand the role of RAP1GAP in the differential response of primary and metastatic melanoma cells, we first evaluated RAP1GAP expression in matched set of primary and LNM cells. Although RAP1GAP protein levels appeared to be higher in metastatic melanoma cells in one set of matched primary and metastatic lines, similar increase in metastatic cells was not seen in a second matched set of primary and metastatic cells (Fig. 4A). EPAC inhibition, appeared to increase RAP1GAP expression in metastatic melanoma cells and decrease its levels in primary melanoma cells (Supp Fig. S7). Next, we used lentiviral RAP1GAP shRNA to assess the effect of RAP1GAP knockdown (RAP1GAP-KD) on active RAP1 levels. Interestingly, in both matched primary and metastatic melanoma cells, RAP1GAP-KD resulted in a slight increase (1.09 and 1.25-fold change, respectively) in active RAP1 (Rap1-GTP) (Fig. 4B). RAP1GAP-KD did not rescue downregulation of RAP1-GTP in primary melanoma by treatment with ESI-09 whereas RAP1GAP-KD partially dampened the effect of ESI-09 on RAP1-GTP levels in LNM cells (Fig. 4B).

Next, we tested the effect of RAP1GAP-KD on the differential growth inhibition caused by EPAC inhibition. RAP1GAP-KD alone had no effect on the growth of either primary or metastatic melanoma cells. Consistent with the biochemical data, in primary melanoma cells RAP1GAP-KD did not rescue growth inhibition caused by EPAC inhibition, but RAP1GAP-KD appeared to sensitize metastatic melanoma cells to EPAC inhibition (Fig. 4C). These data suggest that the levels of RAP1-GTP inactivating protein RAP1-GAP do not correlate with the differential effects of EPAC inhibition on primary and metastatic melanoma cells.

Subcellular distribution of EPAC, active RAP1 and RAP1GAP proteins

It is known that subcellular localization of EPAC, specifically different isoforms of EPAC2, determine its physiological functions [27]. Therefore, we investigated whether differential role of EPAC and RAP1GAP proteins in primary and metastatic melanoma is due to differences in their subcellular localization (Fig. 4D). In primary melanoma cells, EPAC1 was enriched predominantly in cytosolic fraction whereas in metastatic melanoma cells it was localized in both cytosolic and membrane fractions. In both primary and metastatic

cells, EPAC2 appears to be distributed in cytosolic, membrane, and nuclear fractions with the highest amounts in nuclear fractions. Interestingly, active RAP1 (RAP1-GTP) was enriched in nuclear fraction in both primary and metastatic cells consistent with the preferential localization of EPAC2. In both primary and metastatic melanoma cells, bulk of RAP1GAP is present in the cytosolic fraction with smaller amounts localized in membranes. Thus, although membrane localization of RAP1-GTP appears to be different in primary and metastatic cells, these differences in subcellular distribution of EPAC, RAP1 and RAP1GAP do not correlate with the differential response of primary and metastatic cells to EPAC inhibition.

EPAC activity negatively regulates AKT

Delayed cell cycle progression and growth inhibition of primary melanoma cells by EPAC inhibition was not associated with inhibition of MAP kinase activity. Phosphorylated ERK1/2 remained unchanged in ESI-09 treated primary melanoma cells. ESI-09 treated metastatic melanoma cells, however, showed an increase in pERK1/2 consistent with growth stimulation (Fig 5A). Interestingly, ESI-09 treatment resulted in increased pAKT (Ser473) levels in primary melanoma cells but not in metastatic melanoma cells (Fig 5A). In the matched melanoma primary and LNM cell lines, EPAC inhibition resulted in increased AKT phosphorylation in primary (WM115) and LNM (WM266-4 and WM239-A) cells but not WM165-cells (Fig 5A). As shown in (Supp Fig. S8A), ESI-09 treatment-induced increase in pAKT levels was not dependent on cell density. These data show that EPAC signaling acts as a negative regulator of AKT activation.

Inhibition of primary melanoma cell growth by ESI-09 is dependent on AKT activation

Time course analysis of the effect of ESI-09 on the activation AKT in primary melanoma cell line WM1552C showed a gradual increase in pAKT levels between 8-24 hours of treatment with ESI-09 followed by a decrease in both total and pAKT levels at 48hour treatment (Fig. 5B). The decrease in total and pAKT between 24 and 48 hours appeared to coincide with the loss of rescue from growth inhibition by ESI-09 (see Supp Fig. S1A). To investigate the role of pAKT in the growth inhibition of primary melanoma cells by ESI-09, we evaluated the effect of inhibitor of AKT phosphorylation KRX-0401 (Fig. 5C) and an inhibitor of AKT activity AZD5363 (Fig. 5D) on reversibility of the effect of ESI-09. Replacing the medium containing ESI-09 with inhibitor-free medium after 24h treatment partially reversed the inhibitory effect of ESI-09 on cell growth (Fig 5C and D). However, addition of inhibitor of AKT phosphorylation KRX-0401 or AKT activity AZD5363 in the replacement medium prevented, in a dose-dependent manner, the partial rescue from growth inhibition caused by ESI-09 (Fig 5C and D). Treatment of metastatic melanoma cell line MRA6 with ESI-09 alone 24h stimulated their growth (similar to data shown in Fig 1B) and removal of ESI-09 decreases the growth stimulation. However, upon addition of AKT inhibitors to the ESI-09-free medium there was a dose-dependent stimulation of the growth of MRA6 cells. Western blot analysis of AKT levels showed an increase in pAKT levels in cells treated with ESI-09, but removal of the EPAC inhibitor decreased the levels of pAKT (Supp Fig S8B).

EPAC regulates AKT/mTOR signaling in melanoma

Western blot analysis of matched primary and LNM cell lines treated with ESI-09 for 24 hours showed upregulation of phosphorylation of AKT at Thr308 and Ser473 (Fig. 6). AKT phosphorylation in the matched set of primary and LNM cell lines appeared to progressively become refractory to ESI-09 treatment. PDK1 phosphorylates Thr308 on AKT whereas is mTORC2 is known to phosphorylated Ser473. We investigated the effect of EPAC inhibition on the subunits of mTOR complexes, mTORC1 and mTORC2. Raptor is a component of mTORC1 and Rictor is a component of mTORC2 [28]. In ESI-treated cells, the inhibitory phosphorylation of Rictor (Rictor-Thr1135) was downregulated. This simultaneous activation of Rictor (as seen by downregulation of inhibitory phosphorylation) and AKT (AKT-Ser473) suggest that mTORC2 regulates phosphorylation of AKT in ESI-09 treated cells. On the other hand, ESI-09 treatment increased the inhibitory phosphorylation of Raptor (Ser792) in primary melanoma cells and caused progressively less upregulation in the matched LNM cells. Raptor ser792 phosphorylation is known to be regulated by the cellular energy sensor AMP-activated protein kinase (AMPK), a negative regulator of mTORC1. Therefore, we examined the levels of Thr172 phosphorylation of AMPK, which stimulates AMPK activity. ESI-09 treatment decreased the phosphorylation of AMPK (as seen by two bands phosphorylation) with a slight increase in the lower band in primary and LNM cells WM266-4 and WM239A whereas this decrease was not detectable in LNM cell line WM165-1. These data suggest inhibition of EPAC signaling leads to activation of AMPK, which inhibits Raptor and the activity of mTORC1. Inhibition of mTORC1 activity in ESI-09 treated cells is also evident from decreased phosphorylation of its substrates, p70 S6 kinase, a regulator of G1/S cell cycle progression, and 4EBP1, a regulator of protein translation. In ESI-09 treated WM115 primary melanoma cells and WM266-4 LNM cells, there was a faster migrating band for p70S6K (a less phosphorylated protein) [29]. This faster migrating p70S6K becomes progressively less pronounced in WM239-A and WM165-1 LNM cells. p85S6K protein also shows similar change upon ESI-09 treatment. mTOR first phosphorylates Thr37 and Thr46 on 4E-BP1 (eIF-4E-binding protein 1) complexed with eIF4E (eukaryotic initiation factor). Then, extracellular stimuli-induced phosphorylation of Ser65 and Thr70 is known to result in the release from eIF4E and stimulation of translation [30]. Interestingly, treatment with ESI-09 appears to shift the expression of β and γ isoforms 4E-BP1 to α isoform [31, 32] and this shift became progressively less pronounced and not detected in WM165-1 cells. In addition, we noted progressive increase in Thr70 phosphorylation and decrease in Ser65 phosphorylation of the lower 4E-BP1 band. p70 S6 kinase is also known to phosphorylate Rictor at Thr1135 [33, 34]. This inhibitory phosphorylation points to mTORC1 causing feedback inhibition of mTORC2 and hence inhibition of AKT. These data suggest a feedback and regulation of AKT and growth inhibition in ESI-treated primary melanoma cells.

EPAC regulates mitochondrial reactive oxygen species (mROS) production

Mitochondrial reactive oxygen species are produced as byproducts of mitochondrial metabolism. mROS is known to have both pro- and anti-tumorigenic effects [35, 36]. Therefore, we evaluated the role of EPAC signaling in mitochondrial ROS production. We measured the production of mROS in control and ESI-09-treated cells (Fig. 7A) using MitoSOX Red, a mitochondrial superoxide indicator. ESI-09 treatment caused a 4-fold

increase in mROS production in WM115 and a slightly less increase (2-to-3 fold) in WM266-4 (Fig. 7B). Other LNM linesWM239A and WM165-1 and the distant organ metastases lines MRA5 and MRA6 did not show any change in mROS production upon EPAC inhibition.

EPAC regulates oxidative phosphorylation and glycolysis in primary melanoma

Since EPAC regulates the AMPK and mTOR signaling pathway, is a critical regulator of glycolysis and mitochondrial function, we investigated the effect of ESI-09 on cellular and mitochondrial energy. We assayed oxygen consumption (mitochondrial respiration) and extracellular acidification (glycolysis) rates using the Seahorse Cell Energy Phenotype test performed on the Seahorse Extracellular Flux Analyzer before and after addition of a stressor mix consisting of the compounds, FCCP and oligomycin (Fig. 7C). FCCP is an uncoupling agent that depolarizes the mitochondrial membrane potential and drives oxygen consumption by mitochondria. Oligomycin, an ATP synthase inhibitor, drives the cell to synthesize ATP by glycolysis, hence increasing the extracellular acidification rate. Basal readings were obtained before the addition followed by maximal readings obtained after the addition of the stressor. In the primary cell line WM115, treatment with ESI-09 resulted in a complete inhibition of both basal and maximal mitochondrial respiration. In the LNM cell lines WM266-4, WM239A and WM165-1, a progressively decreasing magnitude of inhibition of basal respiration was noted.

Interestingly, treatment with ESI-09 also caused approximately 50% decrease of basal and maximal glycolysis in the primary cell line WM115. These data show that EPAC promotes survival and growth of primary melanoma cells by regulating both oxidative phosphorylation and glycolysis. Our data also suggest that metabolic adaptation that occurs during tumor progression (including lymphatic spread) progressively relieves the metastatic cells from this dependency on EPAC signaling for their survival. Overall, we propose that by regulating AKT and AMPK activities, EPAC-RAP1 signaling regulates mTORC1 signaling that in turn regulates critical cellular activities such as protein translation, cell glycolysis, mitochondrial ROS production and cycle progression. While primary melanoma cells are critically dependent on EPAC-RAP1-mTORC1, this dependency appears to be progressively lost during metastatic progression. (Fig. 7D).

Prognostic significance of EPAC signaling

To investigate the prognostic value of EPAC1/2 signaling, we queried the Cancer Genome Atlas (TCGA) Firehose Legacy melanoma dataset. This dataset consists of tumor mRNA expression and patient follow data for a cohort of 479 patients. We queried these samples for expression of RAPGEF3, RAPGEF4, RAP1GAP, and mTOR mRNA (Supp Fig. S9). Among the above EPAC signaling protein mRNAs, we found significantly different (i.e., higher in metastatic tumors, $p<0.001$) expression of only RAP1GAP in the metastatic tumors compared primary melanoma tumors (Supp Fig. S9A). Furthermore, among the 86 patients diagnosed with primary melanoma (of a total of 459 patients), high expression of RAPGEF3, RAPGEF4 (highest quartile) in primary melanoma tumors was associated with significantly shorter disease-free survival (HR=2.87, $p= 0.008$ for RAPGEF3 and HR=2.78, $p=0.006$ for RAPGEF4) whereas there was no association of RAP1GAP and

mTOR expression with disease free survival (Supp Fig. S9B). Taken together with our *in vitro* findings on the role of EPAC signaling in the matched primary LNM cells, these data support the notion that higher EPAC signaling in primary melanoma promotes tumor growth and progression.

Discussion

In this study, we show that EPAC signaling promotes the growth and survival of primary melanoma cells by regulating cell cycle progression, suppression mROS production, maintenance of both glycolysis and oxidative phosphorylation. These functions of EPAC appear to be mediated, paradoxically, by both inhibition of AKT activation and stimulation of mTORC1 activity. Employing genetically matched (i. e., isolated form the same patient) series of primary and metastatic melanoma cells, we show that this requirement for EPAC signaling for growth is progressively lost and could even be inhibit their growth of unrelated distant organ metastatic melanoma cells.

The cAMP analog 8-CPT-2-O-Me-cAMP, an activator of EPAC, was shown to induce proliferation of A375 metastatic melanoma cell line by upregulation of b-Raf/ERK and mTOR signaling [37]. Similarly, in other melanoma cell lines this cAMP analog was reported to activate both RAP1 and ERK [38]. In our study we employed multiple independently derived primary and metastatic cell lines to show that EPAC inhibition reproducibly inhibits the growth of only primary melanoma cells independent of the oncogenic driver mutation they harbor and may slightly stimulate the growth of distant organ metastatic cells. Consistent with this, our experiments also showed that treatment with the cAMP analog inhibited the growth metastatic melanoma cells. Interestingly, growth of primary melanoma cells is not affected by treatment with 8-CPT-2-O-Me-cAMP suggesting that EPAC is maximally activated in primary melanoma cells. On the other hand, treatment with Rp-8-bromo-Cyclic AMP, an antagonist of cAMP-dependent protein kinase PKA, inhibited the growth of primary and LNM cells but not metastatic cells.

Although both EPAC1 and EPAC2 are known to act similarly in the context of RAP1 activation, they also appear to have distinct physiological functions [39]. In the context of cancer, for example, in prostate cancer cells, EPAC1 was shown to promote cell proliferation and survival by upregulating Ras-MAPK, and PI3-kinase-Akt-mTOR signaling [37], whereas in H1299 lung cancer cells, Epac2 appears to also activate Rap1A-Akt pathway appears to regulate cisplatin-induced apoptosis [20]. To investigate the relative roles of EPAC1 and EPAC2, we employed both EPAC2-selective inhibitor (ESI-05) and EPAC1/2 inhibitor (ESI-09), and siRNA-mediated knockdown (KD). We noted that either treatment with EPAC2-selective inhibitor alone or transfection with EAPC2 siRNA inhibited the growth primary melanoma cell line WM115, transfection with EPAC1 siRNA also caused growth inhibition, albeit to a significantly less extent.

RAP1-GTP levels are regulated by the activity of EPAC, which is a RAP guanosine exchange factor RAPGEF and RAP1GAP, a GTP hydrolyzing enzyme [40]. In melanoma cells, downregulation of Rap1GAP via promoter hypermethylation was proposed to promote melanoma cell proliferation, survival, and migration [41]. Our analysis of TCGA dataset

for RAP1GAP mRNA in primary and metastatic tumors is consistent with this notion. Interestingly, western blot analysis of RAP1GAP protein showed the opposite pattern, i. e., higher RAP1GAP in LNM cell lines compared to their primary counterparts. Similarly, while overexpression of Rap1GAP was shown to block Rap1activation and ERK phosphorylation [41], in our studies, although RAP1GAP KD (by shRNA lentivirus) slightly increased active RAP1-GTP in both primary and LNM melanoma, it did not affect the growth of primary or metastatic cells. Therefore, it is possible that EPAC regulates melanoma cell proliferation through RAP1-independnet mechanisms. Cyclic AMP and Rap1-indepenet effect of Epac1 in neurite outgrowth have been reported [42].

The role of EPAC signaling in cell cycle progression has been previously documented. In MCF-7 breast cancer cells, EPAC1 was shown to interact A-kinase anchoring protein 9 (AKAP9) and inhibition of EPAC with ESI-09 arrest them at sub-G1 phase of the cell cycle and induce apoptosis by destabilization of AKAP9 [43]. Interestingly, although our studies also show a role for EPAC signaling in cell cycle progression and cell survival, this occurs selectively in primary melanoma cells but not metastatic cells. This is the first demonstration of progressive loss of dependency on EPAC in LNM cells and a differential role of EPAC signaling in primary vs. metastatic cancer cells.

We previously reported that the differences in the effect of EPAC inhibition on the growth of primary and metastatic melanoma cells is not due to differential role of EPAC in MAPK (i. e., MEK1/2-ERK1/2) signaling [22]. In this study, we also show that downregulation of cyclin D1 and inhibition of cell cycle progression by the EPAC inhibitor is not accompanied by downregulation of MAPK pathway. Similarly, treatment with the EPAC inhibitor ESI-09 was shown to inhibit proliferation of ovarian cancer cells *in vitro* and *in vivo* through inactivation of Cyclin D1/CDK4 independent of MAPK pathway inhibition [44].

AKT-mTOR signaling plays a key role in cell cycle, cell survival and cellular energy metabolism [45, 46]. In genetic mouse models, mTORC1 activation has been shown to block BRAF oncogene-induced growth arrest but not sufficient for melanoma tumor development suggesting that dependence on EPAC regulated mTORC1 activation presumably is a late event in melanoma tumorigenesis [47]. An interesting finding in our studies is that EPAC signaling acts as an inhibitor of AKT Ser473 phosphorylation and appears simultaneously to upregulate mTORC1 signaling. It is known that mTOR activation inhibits PI3K signaling and AKT phosphorylation via negative feedback. Accordingly, pharmacological inhibition of mTORC1 and loss of this negative feedback on PI3K signaling caused increased AKT phosphorylation [46, 48]. In this context, although ESI-09 appears to act like mTOR inhibitor rapamycin and causes increases AKT phosphorylation in primary melanoma cells (but not in metastatic cells), this increased AKT phosphorylation does not blunt the antiproliferative effects of mTORC1 inhibition. These data indicate a stringent requirement of mTORC1 activity for the survival of primary melanoma cells.

A role for mTORC1 signaling in the reprogramming that underlies escape from glycolytic addiction has been widely recognized. Active mTORC1 has been shown facilitate escape from glycolytic addition of cancer cells. Accordingly, a combined inhibition of glycolysis and mTORC1 signaling are required to disrupt metabolic reprogramming in tumor cells

and inhibited their growth [49–51]. Metabolic rewiring of melanoma cells is known to be associated with tumor progression [52]. Metastasizing melanomas appear to undergo reversible metabolic changes that increase their capacity to withstand oxidative stress during metastasis [53]. On the other hand, administration of antioxidants was shown to significantly increase the number of lymph node and lung metastases without affecting the growth of primary tumor [54]. In this context, a role for EPAC-RAP1 in cancer cell energy metabolism has been previously reported. In a 3-D cell culture model, EPAC1 has been implicated in oncogenesis of mammary epithelial cells by stimulating glycolysis [55]. In this study we show that EPAC signaling is required for maintenance of both glycolysis and oxidative phosphorylation. This requirement is progressively lost in LNM cells suggesting that EPAC-mediated mechanisms are involved in the metabolic adaptation of melanoma during tumor progression.

Oxidative stress, through the production of reactive oxygen species (ROS), has been proposed as a key regulator of cancer development and progression [56]. Reactive oxygen species (ROS) also plays a crucial role in melanoma pathophysiology [57]. Pharmacological stimulation of Epac-Rap signaling by 8-pCPT-2’-O-Me-cAMP has been shown to reduce ROS production (specifically, mitochondrial superoxides) in the tubular epithelium [58].

Mitochondrial oxidative metabolism is suppressed to lower ROS generation. After reaching Mitochondrial redox metabolism is also known to play a role in metabolic adaptation during tumor progression according to the stage of progression. the distant organ, the intrinsic metabolic limitations of the target site influence their adaptation to the new environment [59]. Epac2-Rap1 signaling has also been shown to regulate mitochondrial ROS production in myocardial arrhythmia susceptibility [60]. In this study we show that EPAC inhibits mROS production in primary melanoma cells and this EPAC dependency to quench mROS is abolished with tumor progression.

In summary, our study shows that in primary melanoma cells EPAC signaling plays a critical role in promoting cell survival and proliferation through activation of mTORC1. EPAC also is involved in regulating mROS production and both glycolysis and oxidative phosphorylation (Fig. 7D). This dependency on EPAC signaling for survival and growth appears to progressively diminish as melanoma cells migrate to lymph nodes and completely lost in the distant organ metastatic cells. Based on these data, we propose high EPAC activity promotes primary melanoma tumor growth and facilitates acquisition of metastatic competence. Consistent with this notion, higher EPAC expression in primary melanoma appear to correlate with shorter disease-free survival. Taken together, our studies highlight EPAC as a potential target for prevention of tumor progression. Understanding the molecular basis for the dependency of primary melanoma on EPAC signaling could open new avenues for treatment of patients with advanced melanoma.

Supplementary Material

Refer to Web version on PubMed Central for supplementary material.

ACKNOWLEDGEMENTS

This research was supported by VA Merit Review Award I01BX004921 (to VS), and in part by the NIAMS Skin Disease Research Center grant P30AR066524, and the Department of Defense grant W81XWH-18-PRCRP-IASF (CA181014) (to VS), VA Merit Review Awards I01BX001008 and I01CX001441 (to NA).

REFERENCES

1. Schadendorf D, et al. , Melanoma. Nature Reviews Disease Primers, 2015: p. 15003.
2. Balch CM, et al. , Final version of 2009 AJCC melanoma staging and classification. J Clin Oncol, 2009. 27(36): p. 6199–206. [PubMed: 19917835]
3. Shain AH and Bastian BC, From melanocytes to melanomas. Nat Rev Cancer, 2016. 16(6): p. 345–58. [PubMed: 27125352]
4. Sleeman J, Schmid A, and Thiele W, Tumor lymphatics. Semin Cancer Biol, 2009. 19(5): p. 285–97. [PubMed: 19482087]
5. Leong SP, et al. , Cutaneous melanoma: a model to study cancer metastasis. J Surg Oncol, 2011. 103(6): p. 538–49. [PubMed: 21480247]
6. Gershenwald JE, et al. , Melanoma staging: Evidence-based changes in the American Joint Committee on Cancer eighth edition cancer staging manual. CA Cancer J Clin, 2017. 67(6): p. 472–492. [PubMed: 29028110]
7. Ubellacker JM, et al. , Lymph protects metastasizing melanoma cells from ferroptosis. Nature, 2020. 585(7823): p. 113–118. [PubMed: 32814895]
8. Rodriguez CI, et al. , EPAC-RAP1 Axis-Mediated Switch in the Response of Primary and Metastatic Melanoma to Cyclic AMP. Mol Cancer Res, 2017. 15(12): p. 1792–1802. [PubMed: 28851815]
9. Roscioni SS, Elzinga CR, and Schmidt M, Epac: effectors and biological functions. Naunyn Schmiedebergs Arch Pharmacol, 2008. 377(4–6): p. 345–57. [PubMed: 18176800]
10. Ichikawa H, et al. , Overexpression of exchange protein directly activated by cAMP-1 (EPAC1) attenuates bladder cancer cell migration. Biochem Biophys Res Commun, 2018. 495(1): p. 64–70. [PubMed: 29111327]
11. Lakhter AJ and Naidu SR, Cyclic AMP-Epac signaling pathway contributes to repression of PUMA transcription in melanoma cells. Melanoma Res, 2017. 27(5): p. 411–416. [PubMed: 28489680]
12. Baljinnyam E, et al. , Exchange protein directly activated by cyclic AMP increases melanoma cell migration by a Ca2+-dependent mechanism. Cancer Res, 2010. 70(13): p. 5607–17. [PubMed: 20551063]
13. Baljinnyam E, et al. , Epac1 increases migration of endothelial cells and melanoma cells via FGF2-mediated paracrine signaling. Pigment Cell Melanoma Res, 2014. 27(4): p. 611–20. [PubMed: 24725364]
14. Baljinnyam E, et al. , Epac1 promotes melanoma metastasis via modification of heparan sulfate. Pigment Cell Melanoma Res, 2011. 24(4): p. 680–7. [PubMed: 21539721]
15. Baljinnyam E, et al. , Gbetagamma subunits inhibit Epac-induced melanoma cell migration. BMC Cancer, 2011. 11: p. 256. [PubMed: 21679469]
16. Almahariq M, et al. , A novel EPAC-specific inhibitor suppresses pancreatic cancer cell migration and invasion. Mol Pharmacol, 2013. 83(1): p. 122–8. [PubMed: 23066090]
17. Rangarajan S, et al. , Cyclic AMP induces integrin-mediated cell adhesion through Epac and Rap1 upon stimulation of the beta 2-adrenergic receptor. J Cell Biol, 2003. 160(4): p. 487–93. [PubMed: 12578910]
18. Bastian P, et al. , The inhibitory effect of norepinephrine on the migration of ES-2 ovarian carcinoma cells involves a Rap1-dependent pathway. Cancer Lett, 2009. 274(2): p. 218–24. [PubMed: 18849110]
19. Sun DP, et al. , EPAC1 overexpression is a prognostic marker and its inhibition shows promising therapeutic potential for gastric cancer. Oncol Rep, 2017. 37(4): p. 1953–1960. [PubMed: 28260059]

20. Park JY and Juhnn YS, cAMP signaling increases histone deacetylase 8 expression via the Epac2-Rap1A-Akt pathway in H1299 lung cancer cells. Exp Mol Med, 2017. 49(2): p. e297. [PubMed: 28232663]
21. Garg J, et al. , Catecholamines facilitate VEGF-dependent angiogenesis via beta2-adrenoceptor-induced Epac1 and PKA activation. Oncotarget, 2017. 8(27): p. 44732–44748. [PubMed: 28512254]
22. Rodriguez CI, EPAC-Rap1 axis-mediated switch in the response of primary and metastatic melanoma cells to cyclic AMP signaling. Under revision, 2017.
23. Gao J, et al. , Integrative analysis of complex cancer genomics and clinical profiles using the cBioPortal. Sci Signal, 2013. 6(269): p. pl1.
24. Cerami E, et al. , The cBio cancer genomics portal: an open platform for exploring multidimensional cancer genomics data. Cancer Discov, 2012. 2(5): p. 401–4. [PubMed: 22588877]
25. Lotfi S, et al. , Role of the exchange protein directly activated by cyclic adenosine 5'-monophosphate (Epac) pathway in regulating proglucagon gene expression in intestinal endocrine L cells. Endocrinology, 2006. 147(8): p. 3727–36. [PubMed: 16644915]
26. Herlyn M, et al. , Primary melanoma cells of the vertical growth phase: similarities to metastatic cells. J Natl Cancer Inst, 1985. 74(2): p. 283–9. [PubMed: 3856042]
27. Qiao J, et al. , Cell cycle-dependent subcellular localization of exchange factor directly activated by cAMP. J Biol Chem, 2002. 277(29): p. 26581–6. [PubMed: 12000763]
28. Manning BD and Toker A, AKT/PKB Signaling: Navigating the Network. Cell, 2017. 169(3): p. 381–405. [PubMed: 28431241]
29. Laser M, et al. , Differential activation of p70 and p85 S6 kinase isoforms during cardiac hypertrophy in the adult mammal. J Biol Chem, 1998. 273(38): p. 24610–9. [PubMed: 9733756]
30. Gingras AC, et al. , Regulation of 4E-BP1 phosphorylation: a novel two-step mechanism. Genes Dev, 1999. 13(11): p. 1422–37. [PubMed: 10364159]
31. Ayuso MI, et al. , New hierarchical phosphorylation pathway of the translational repressor eIF4E-binding protein 1 (4E-BP1) in ischemia-reperfusion stress. J Biol Chem, 2010. 285(45): p. 34355–63. [PubMed: 20736160]
32. Woodcock HV, et al. , The mTORC1/4E-BP1 axis represents a critical signaling node during fibrogenesis. Nat Commun, 2019. 10(1): p. 6. [PubMed: 30602778]
33. Dibble CC, Asara JM, and Manning BD, Characterization of Rictor phosphorylation sites reveals direct regulation of mTOR complex 2 by S6K1. Mol Cell Biol, 2009. 29(21): p. 5657–70. [PubMed: 19720745]
34. Baturcam E, et al. , MEK inhibition drives anti-viral defence in RV but not RSV challenged human airway epithelial cells through AKT/p70S6K/4E-BP1 signalling. Cell Commun Signal, 2019. 17(1): p. 78. [PubMed: 31319869]
35. Sullivan LB and Chandel NS, Mitochondrial reactive oxygen species and cancer. Cancer Metab, 2014. 2: p. 17. [PubMed: 25671107]
36. Samper E, Nicholls DG, and Melov S, Mitochondrial oxidative stress causes chromosomal instability of mouse embryonic fibroblasts. Aging Cell, 2003. 2(5): p. 277–285. [PubMed: 14570235]
37. Misra UK and Pizzo SV, Epac1-induced cellular proliferation in prostate cancer cells is mediated by B-Raf/ERK and mTOR signaling cascades. J Cell Biochem, 2009. 108(4): p. 998–1011. [PubMed: 19725049]
38. Gao L, et al. , Ras-associated protein-1 regulates extracellular signal-regulated kinase activation and migration in melanoma cells: two processes important to melanoma tumorigenesis and metastasis. Cancer Res, 2006. 66(16): p. 7880–8. [PubMed: 16912161]
39. Robichaux WG 3rd and Cheng X, Intracellular cAMP Sensor EPAC: Physiology, Pathophysiology, and Therapeutics Development. Physiol Rev, 2018. 98(2): p. 919–1053. [PubMed: 29537337]
40. Hattori M and Minato N, Rap1 GTPase: functions, regulation, and malignancy. J Biochem, 2003. 134(4): p. 479–84. [PubMed: 14607972]

41. Zheng H, et al. , Down-regulation of Rap1GAP via promoter hypermethylation promotes melanoma cell proliferation, survival, and migration. Cancer Res, 2009. 69(2): p. 449–57. [PubMed: 19147557]
42. Baameur F, et al. , Epac1 interacts with importin β1 and controls neurite outgrowth independently of cAMP and Rap1. Sci Rep, 2016. 6: p. 36370. [PubMed: 27808165]
43. Kumar N, et al. , Role of exchange protein directly activated by cAMP (EPAC1) in breast cancer cell migration and apoptosis. Mol Cell Biochem, 2017. 430(1-2): p. 115–125. [PubMed: 28210903]
44. Gao M, et al. , Epac1 knockdown inhibits the proliferation of ovarian cancer cells by inactivating AKT/Cyclin D1/CDK4 pathway in vitro and in vivo. Med Oncol, 2016. 33(7): p. 73. [PubMed: 27277757]
45. Fruman DA and Rommel C, PI3K and cancer: lessons, challenges and opportunities. Nat Rev Drug Discov, 2014. 13(2): p. 140–56. [PubMed: 24481312]
46. Hanahan D and Weinberg RA, Hallmarks of cancer: the next generation. Cell, 2011. 144(5): p. 646–74. [PubMed: 21376230]
47. Damsky W, et al. , mTORC1 activation blocks BrafV600E-induced growth arrest but is insufficient for melanoma formation. Cancer Cell, 2015. 27(1): p. 41–56. [PubMed: 25584893]
48. Sudarsanam S and Johnson DE, Functional consequences of mTOR inhibition. Curr Opin Drug Discov Devel, 2010. 13(1): p. 31–40.
49. de Padua MC, et al. , Disrupting glucose-6-phosphate isomerase fully suppresses the “Warburg effect” and activates OXPHOS with minimal impact on tumor growth except in hypoxia. Oncotarget, 2017. 8(50): p. 87623–87637. [PubMed: 29152106]
50. Pusapati RV, et al. , mTORC1-Dependent Metabolic Reprogramming Underlies Escape from Glycolysis Addiction in Cancer Cells. Cancer Cell, 2016. 29(4): p. 548–562. [PubMed: 27052953]
51. Boudreau A, et al. , Metabolic plasticity underpins innate and acquired resistance to LDHA inhibition. Nat Chem Biol, 2016. 12(10): p. 779–86. [PubMed: 27479743]
52. Ratnikov BI, et al. , Metabolic rewiring in melanoma. Oncogene, 2017. 36(2): p. 147–157. [PubMed: 27270434]
53. Piskounova E, et al. , Oxidative stress inhibits distant metastasis by human melanoma cells. Nature, 2015. 527(7577): p. 186–91. [PubMed: 26466563]
54. Le Gal K, et al. , Antioxidants can increase melanoma metastasis in mice. Sci Transl Med, 2015. 7(308): p. 308re8.
55. Onodera Y, Nam JM, and Bissell MJ, Increased sugar uptake promotes oncogenesis via EPAC/RAP1 and O-GlcNAc pathways. J Clin Invest, 2014. 124(1): p. 367–84. [PubMed: 24316969]
56. Helfinger V and Schröder K, Redox control in cancer development and progression. Mol Aspects Med, 2018. 63: p. 88–98. [PubMed: 29501614]
57. Obrador E, et al. , Oxidative stress and antioxidants in the pathophysiology of malignant melanoma. Biol Chem, 2018.
58. Stokman G, et al. , Epac-Rap signaling reduces oxidative stress in the tubular epithelium. J Am Soc Nephrol, 2014. 25(7): p. 1474–85. [PubMed: 24511123]
59. Choudhury FK, Mitochondrial Redox Metabolism: The Epicenter of Metabolism during Cancer Progression. Antioxidants (Basel), 2021. 10(11).
60. Yang Z, et al. , Epac2-Rap1 Signaling Regulates Reactive Oxygen Species Production and Susceptibility to Cardiac Arrhythmias. Antioxid Redox Signal, 2017. 27(3): p. 117–132. [PubMed: 27649969]

Implications:

This study establishes loss of dependency on EPAC-mTORC1 signaling as hallmark of primary melanoma evolution and targeting this escape mechanism is a promising strategy for metastatic melanoma.

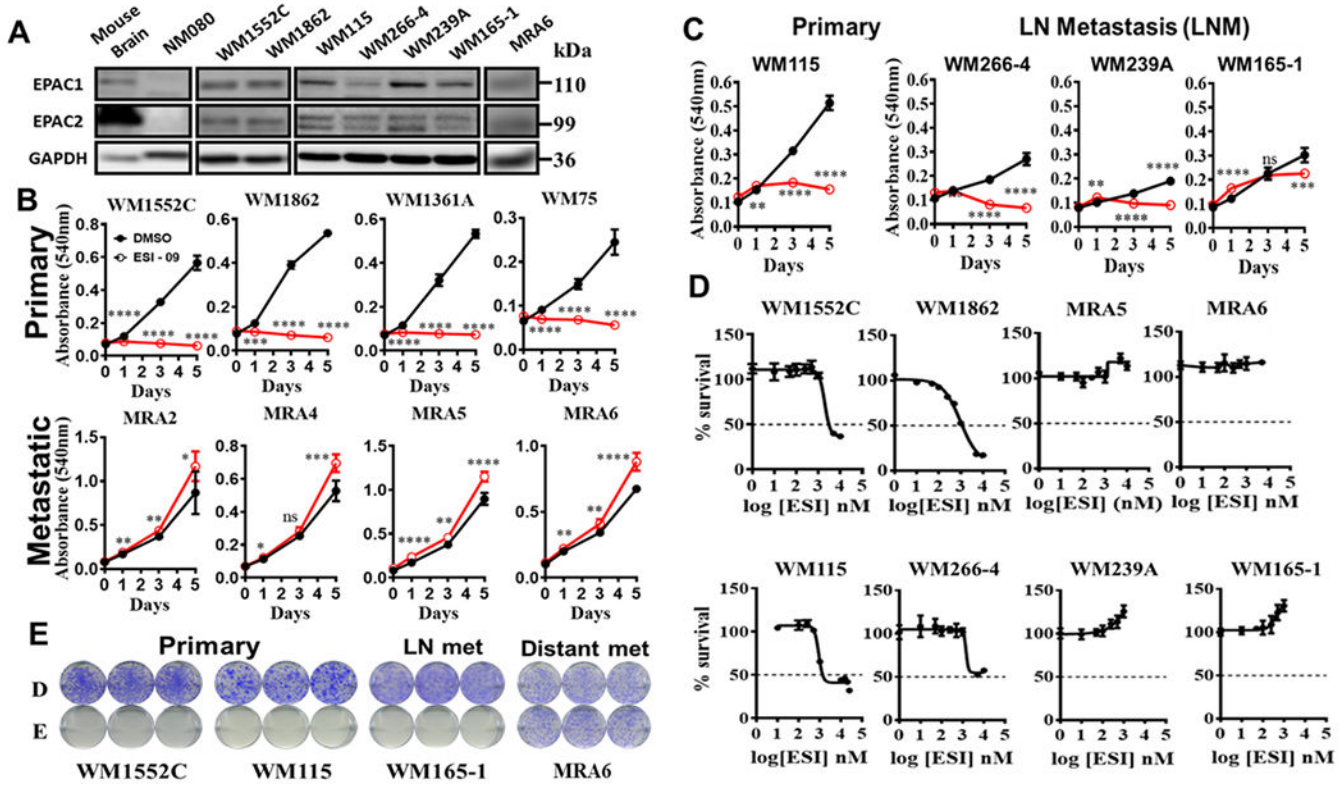

Figure 1: Differential role of EPAC in primary and metastatic melanoma cells

(**A)** Western blot analysis showing endogenous levels of EPAC1 and EPAC2 proteins in mouse brain lysate (positive control), neonatal human primary melanocytes and a panel of primary and metastatic melanoma cells. GAPDH shows equal loading of protein. Numbers on the right indicate the molecular weight (kDa) of the respective proteins. (**B)** Effect of EPAC inhibition on the growth of primary and metastatic melanoma cells. Cells were plated in 6 replicates in 96-well plates and treated with 2.5μM ESI-09 for 5 days. Drug was replenished every 48h and cell number was estimated using MTT assay. **(C)** Effect of pharmacological inhibition of EPAC1/2 on matched primary and metastatic cells established from the same patient. Cells were plated in 6 replicates in 96-well plates and treated with 2.5 μM ESI-09 for 5 days. Data shown as mean ± SD were analyzed by Student's *t*-test. *Indicates p-value ≤0.05; ** ≤0.01; *** ≤0.001 and **** ≤0.0001. **(D)** Dose-response curves for effect of ESI-09 treatment. A panel of primary and metastatic melanoma cells were plated in 6 replicates in a 96-well plate and treated with 10nM-10μM ESI-09. Survival was measured after 72h using MTT assay. Mean ± SD of the replicates normalized to DMSO control are shown. **(E)** Effect of EPAC inhibition on clonogenicity of primary and metastatic melanoma cells. Cells were plated in triplicates in 6-well plates and treated with DMSO or 5μM ESI-09. Media containing drug was replenished every 5 days for 2 weeks. Cells were fixed and stained with crystal violet made in 70% ethanol.

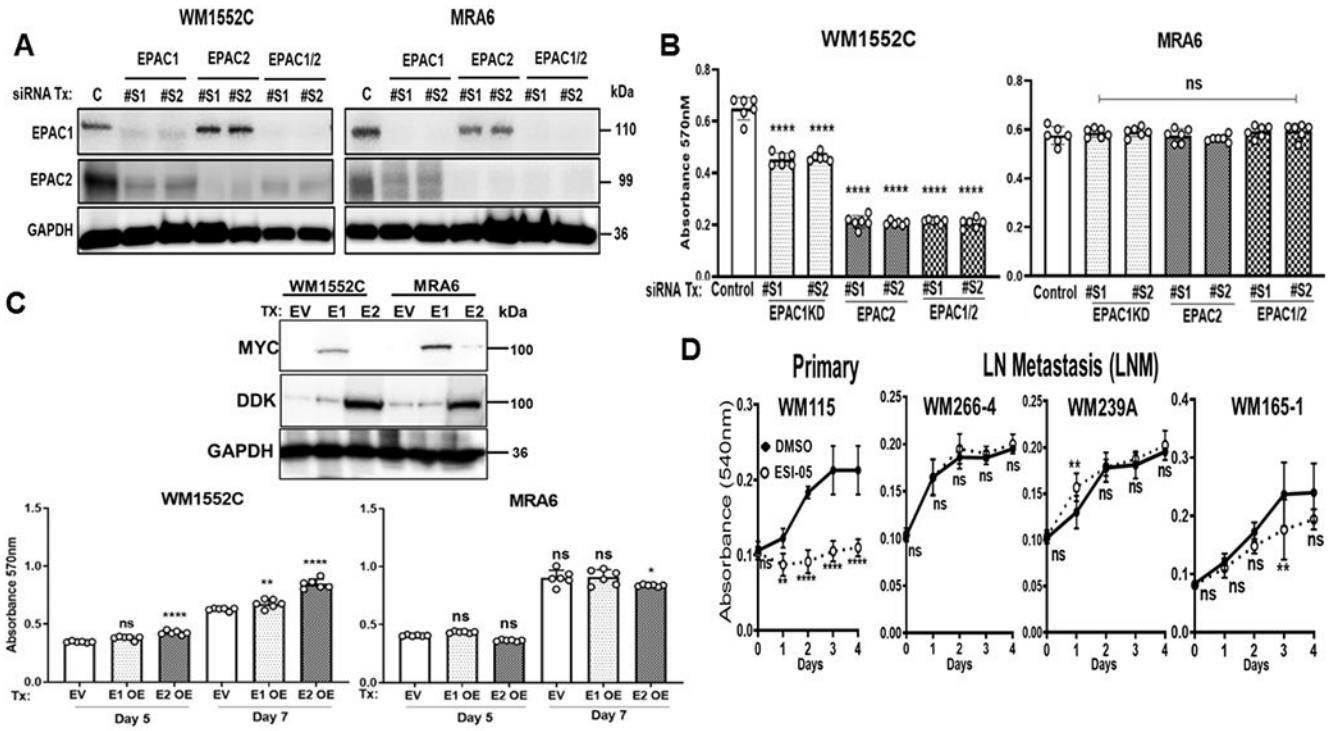

Figure 2: Effect of EPAC1/2 knockdown and overexpression on primary and metastatic melanoma cells.

(**A)** Western blot analysis of EPAC1 and EPAC2 in WM1552C primary and MRA6 metastatic melanoma cells 96h after transfection with control or two different EPAC1, EPAC2 or EPAC1/2 siRNAs. Numbers on the right indicate the molecular weight (kDa) of the respective proteins. (**B)** Effect of EPAC1/2 knockdown on primary (WM1552C) and metastatic (MRA6) cells after 96h of transfection. Data (mean ± SD) from 6 replicates analyzed by unpaired Student's t test are shown. **(C**) Western blot analysis for MYC tagged-EPAC1 and DDK tagged-EPAC2 in WM1552C and MRA6 cells after 5days of transduction. Numbers on the right indicate the molecular weight (kDa) of the respective proteins. MTT assay shows the effect of MYC tagged-EPAC1 and DDK tagged-EPAC2 overexpression on the survival of primary and metastatic melanoma cells after 5- and 7-days post-transduction. Data (mean ± SD) from 6 replicates analyzed by unpaired Student's *t* test are shown. p-values: * indicates $P \leq 0.05$; ** ≤0.01; *** ≤0.001 and **** ≤0.0001. (**D)** Effect of EPAC2 selective inhibitor ESI-05 on the growth of primary and metastatic cells established from the same patient measured using MTT assay. Cells were plated in six replicates in 96-well plates in 6 replicates and treated with 2.5 μM ESI-05. Data (mean ± SD) were analyzed by unpaired Student's *t*-test. * Indicates p-value ≤0.05; ** ≤0.01; *** ≤0.001 and **** ≤0.0001.

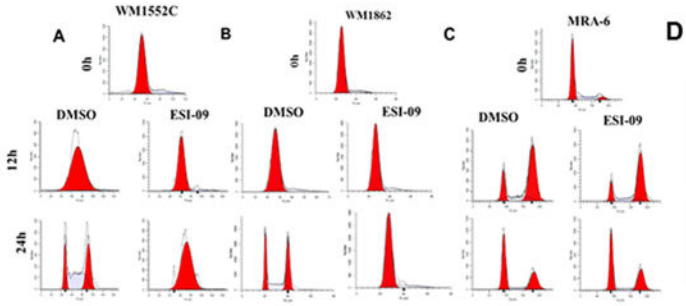

	Primary Melanoma								Metastatic Melanoma			
	WM1552C				WM1862				MRA6			
Treatment	DMSO		ESI-09		DMSO		ESI-09		DMSO		ESI-09	
Time(h)	12hrs	24hrs	12hrs	24hrs	12hrs	24hrs	12hrs	24hrs	12hrs	24hrs	12hrs	24hrs
G1	98.8 ± 2.08	20.78 ± 2.70	**88.78 ± 2.32**	**96.85 ± 1.12**	88.57 ± 0.4	30.37 ± 0.80	86.83 ± 1.32	**82.77 ± 4.39**	16.82 ± 1.67	55.04 ± 0.70	14.15 ± 0.23	**51.72 ± 1.25**
S	1.2 ± 2.08	43.01 ± 4.64	**11.22 ± 2.32**	**3.03 ± 1.23**	11.35 ± 0.53	25.83 ± 0.99	12.52 ± 1.12	**16.29 ± 2.92**	17.09 ± 1.42	10.63 ± 1.48	17.09 ± 0.23	11.22 ± 0.86
G2	0	36.22 ± 2.02	0	**0.09 ± 0.12**	0.07 ± 0.13	43.8 ± 0.72	0.65 ± 0.52	**0.92 ± 1.48**	66.1 ± 0.31	34.33 ± 0.92	**68.75 ± 0.27**	**37.05 ± 0.62**

*The values in bold are statistically significant

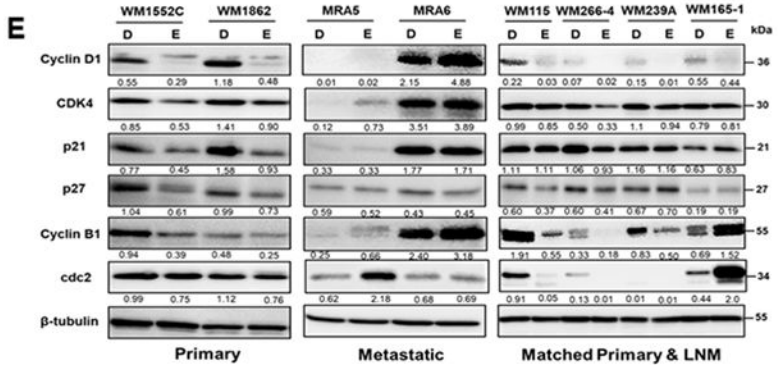

Figure 3: EPAC regulates cell cycle progression in primary but not metastatic melanoma.

(A-D) Effect of EPAC on cell cycle was determined by propidium iodide (PI) staining and flow cytometry analysis. WM1552C, WM1862 and MRA6 cells were plated in triplicates and synchronized using thymidine double block. Cells were treated with DMSO (control) or 5μM ESI-09 post-synchronization and cells were harvested and stained with PI overnight at 0h and after 12 and 24 hours. Flow cytometry was performed using BD Accuri C6.

(E) Western blot analysis showing levels of cell cycle regulatory proteins in primary (WM1552C, WM1862), metastatic (MRA5 and MRA6) and the matched cells (WM115, WM266-4, WM239A, WM165-1) treated with DMSO (control) or ESI-09 for 8h. GAPDH shows equal protein loading. Numbers on the right indicate the molecular weight (kDa) of the respective proteins.

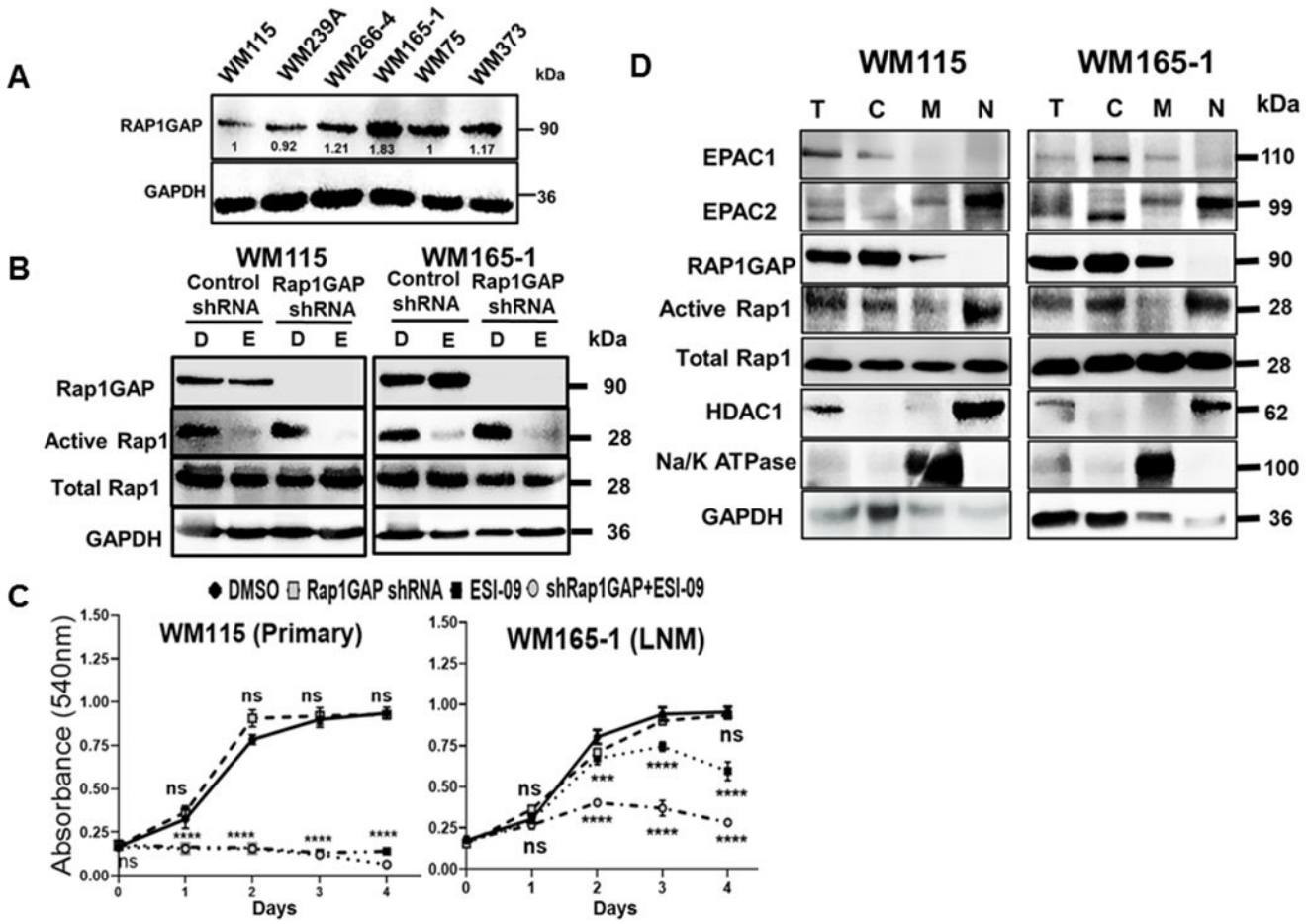

Figure 4: Role of RAP1GAP in growth of primary and metastatic melanoma cells and subcellular distribution of EPAC1/2 signaling proteins.

(A) Western blot analysis showing endogenous levels of RAP1GAP protein in a panel of matched primary and metastatic melanoma cells. GAPDH is used as loading control. Numbers on the right indicate the molecular weight (kDa) of the respective proteins. **(B)** Western blot for validation of RAP1GAP knockdown. Matched primary and metastatic melanoma cells were transduced with RAP1GAP shRNA or scrambled shRNA control lentivirus and selected in puromycin containing medium for 4 days. Protein lysates were analyzed for RAP1GAP, total and active RAP1 (RAP1-GTP). **(C)** Effect of RAP1GAP KD and ESI-09 treatment on the growth of primary and metastatic melanoma cells. Data (mean ± SD) from 3 replicates analyzed by unpaired Student's *t* test are shown. * Indicates p-value ≤0.05; ** ≤0.01; *** ≤0.001 and **** ≤0.0001. **(D)** Western blot showing sub-cellular distribution of EPAC1/2, RAP1-GTP and RAP1GAP in matched primary (WM115) and metastatic (WM165-1) melanoma cells. GAPDH, Na/K-ATPase and HDAC1 were used as makers of cytosolic (C), membrane (M) and nuclear (N) fractions, respectively. Numbers on the right indicate the molecular weight (kDa) of the respective proteins.

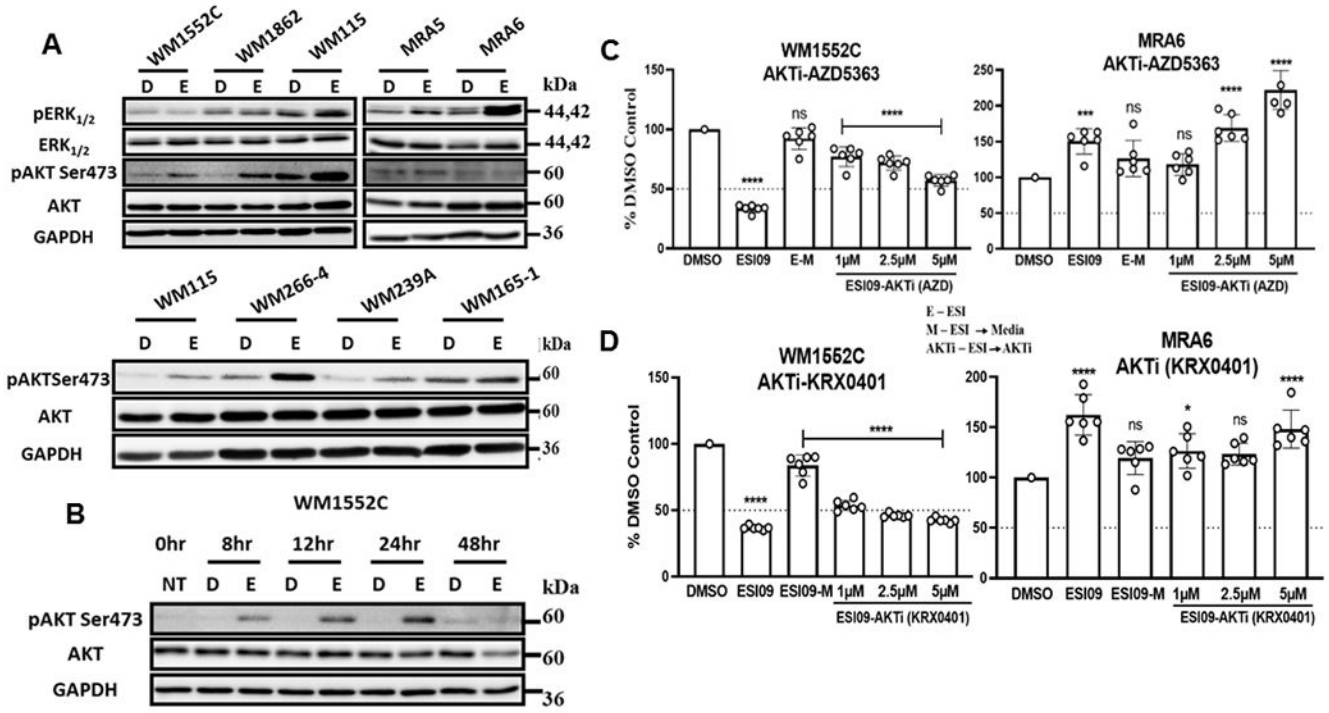

Figure 5: EPAC regulates AKT and mTORC1 signaling

(A) Western blot analysis of primary and metastatic melanoma cells (*top panels*) and matched primary LNM melanoma cells treated for 8h with DMSO (D) and ESI-09 (E) for phosphorylated and total ERK1/2 and AKT. **(B)** Time course of AKT phosphorylation in primary melanoma cell line WM1552C. Western blot analysis of cells treated with ESI-09 for 8-48h. GAPDH shows equal protein loading. Numbers on the right indicate the molecular weight (kDa) of the respective proteins. **(C)** Effect of AKT inhibitors on reversibility of effect of EPAC on WM1552C and MRA6. Cells were plated in 6 replicates in 96-well plates and treated with DMSO or 5μM ESI-09 for 24h. In one set of wells, medium was replaced with ESI-09 containing growth medium, and in a second set of wells, the medium was replaced with medium without ESI-09, and in a third set of well, ESI-09 medium was replaced growth medium containing AKT inhibitors (AKTi– KRX-0401 or AZD5363. Cells were cultured for up to 5 days and cell numbers were estimated using MTT assay and data were analyzed by Student's *t*-test. * Indicates p-value ≤0.05; ** ≤0.01; *** ≤0.001 and **** ≤0.0001. **(D)** Western blot analysis showing levels of pAKT and total AKT in samples treated to DMSO, ESI-09 and AKTi in parallel experiment described in **(C)**. GAPDH shows equal loading of protein. Numbers on the right indicate the molecular weight (kDa) of the respective proteins.

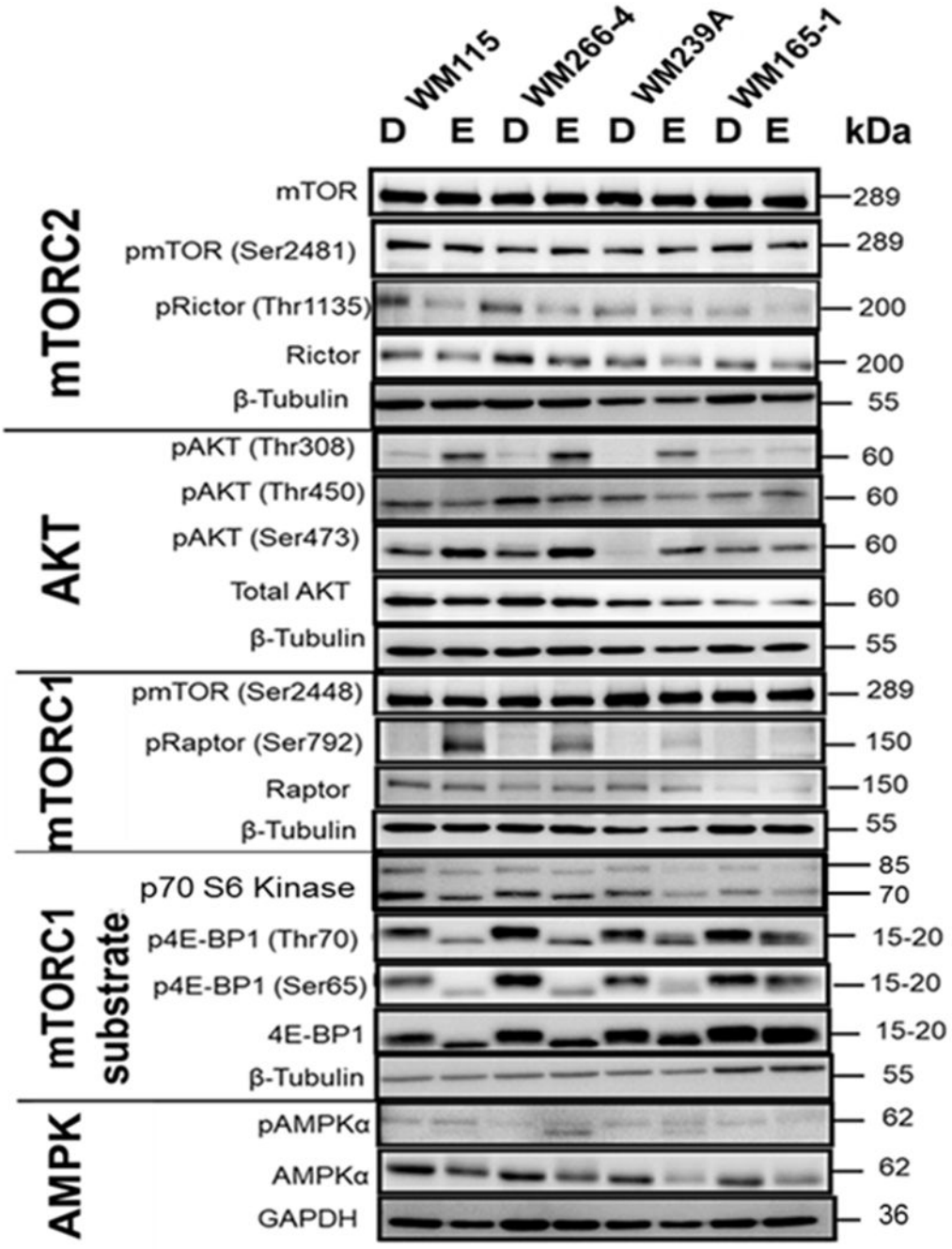

Figure 6: EPAC regulates AMPK, AKT and mTOR signaling.

Western blot analysis of components of the AKT/mTOR signaling pathway in the matched primary and LNM cell lines WM115, WM266-4, WM239A and WM165-1 and the distant organ metastatic cell lines MRA5 and MRA6 after a 24h treatment with DMSO (D) or 2.5 μM ESI-09 (E). Numbers on the right indicate the molecular weight (kDa) of the respective proteins.

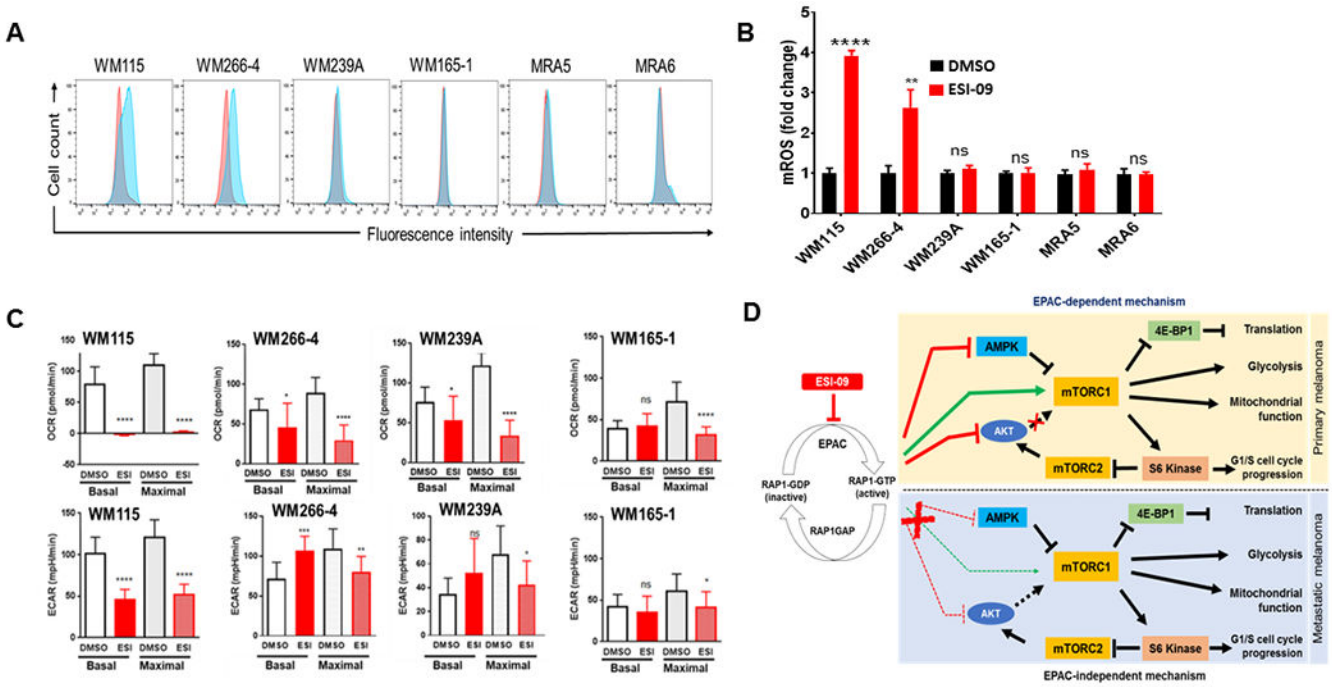

Figure 7: EPAC regulates mROS production and mitochondrial and cellular metabolism.

Effect of pharmacological inhibition of EPAC1/2 on mROS production in the matched primary and LNM melanoma cells and the distant unrelated organ metastatic melanoma cell lines MRA5 and MRA6. Flow cytometry analysis of MitoSOX-Red stained performed using cells harvested 48h after treatment with DMSO or 2.5 μM ESI-09. **(A)** Representative histogram from three replicates with the red peak showing DMSO-treated cells and blue peak showing ESI-treated cells. Data were analyzed was performed using FlowJo. **(B)** Data from three replicates show fold change in mROS levels after ESI-09 treatment. Representative data from two independent experiments are shown. * p-value ≤0.05. ** ≤0.01; *** ≤0.001 and **** ≤0.0001. **(C)** Mitochondrial respiration [measured as oxygen consumption rate (OCR)] and glycolysis [measured as extracellular acidification rate (ECAR)] were assayed by Cell Energy Phenotype test using Seahorse Extracellular Flux Analyzer. This experiment was performed 24 hours after treatment of WM115, WM266-4, WM239A and WM165-1 cells with DMSO or 2.5 μM ESI-09. Basal OCR and ECAR were measured, then stressor mix was added and maximal OCR and ECAR measured. Representative data from two independent experiments are shown. * Indicates p-value ≤0.05; ** P≤0.01; *** P≤0.001 and **** P≤0.0001. **(D)** A schematic for the possible mechanisms of action of EPAC in promoting survival and growth of primary melanoma cells, where mTORC1 is activated by EPAC either directly or through AMPK (green arrows) presumably independent of AKT, which is inhibited by EPAC (red arrow). Dashed lines indicate indirect actions or that it is unknown whether additional steps are required.